GPetrology, Geochemistry and Fractional Modelling Of El-Gidami Neoproterozoic Granitic Rocks, Central Eastern Desert, Egypt.

El Mezayen A.M[1]., Heikal M.A[1]., Omar, S. A[2],. El-Feky M.G[2]., Lasheen S.R[1].

[1]Geologogy Department, Faculty of Science, Al Azher University, Egypt.
[2]Nuclear Material Authority, Egypt.
Elmezayen50@hotmail.com

Abstract: El-Gidami area lies in the Central Eastern Desert of Egypt. This area is composedofamphibolite, oldergranites (OG) and younger granites (YG). The OG is of tonalitic to granodioritic composition with peraluminous nature whereas the Y Ggranitevaries in composition from monzogranite to syenogranite with calc alkaline nature. The OG are enriched in both Sr and Ba but depleted in Rb, whereas the Y Ghave lower Sr and Ba and higher Rb. Both OG and YG are poor in REE. Fractional crystallization and mass balance modeling are used to calculate the amount of sum square of the residuals ($\sum R^2$). The calculation has been performed for granodiorite and the younger granite (monzogranite) of Gabal El-Gidami as one separate system, then granodiorite and the younger granite (syenogranite) of Gabal El-Gidami as another separate system that gives a small value of the residuals which indicates a best fit $\sum R^2$ (0.006 &0.007 respectively).
[El Mezayen A.M., Heikal M.A., Omar, S. A. El-Feky M.G., Lasheen S.R. **Petrology, Geochemistry and Fractional Modelling Of El-Gidami Neoproterozoic Granitic Rocks, Central Eastern Desert, Egypt.** *Nat Sci* 2015;13(7):102-114]. (ISSN: 1545-0740). http://www.sciencepub.net/nature. 12

Key words: El-Gidami, Geochemistry, Fractional modelling and mass balance.

1. Introduction

The basement rocks in the Eastern Desert have been distinguished into three tectono-lithologic domains: North, Central and South Eastern Desert domains (El Ramly, 1972; Stern and Hedge, 1985 and El Gaby, *et al.,* 1988). Gabal El-Gidami lies in the Central Eastern Desert of Egypt south Qena-Safaga road and comprises different rock types of the basement complex besides cover of sandstone.

The Egyptian granitic rocks are classified into two main groups; an older syn-tectonic calc-alkaline granites (OG) referred to as grey granites, and a younger or late to post tectonic granite series (YG) referred to as pink granites (El Ramly and Akaad, 1960; El-Shazly, 1964; El-Ramly, 1972; Sabet *et al.,* 1972; El-Gaby, 1975 and Akaad and Noweir, 1980). The OG are characterized by relatively moderate silica content (≤ 67%), high alumina, high calcium, high soda and less potash content, while theYGare characterized by their high silica content, low calcium content, low soda and high potash (El Shatoury *et al.,* 1984). These younger granites represent the last major magmatic event in the evolution of the crystalline basement of Egypt and belong to the Pan African plutonism.

The pink granitic masses (El-Missikate, El-Gidami and El-Eridiya (are enriched are rich in SiO_2 and total alkalies, and developed in a within plate (El-Mansi, 1993; Abu Dief *et al.,* 1997; Mousa, 2008) that considered as uraniferous granites (Dardier and El-Galy, 2000; Abd El-Nabi, 2001). Mineralization is structurally controlled and is associated with jasperoid veins within granitic pluton (Abd El-Naby, 2007; Hegazy, 2014) especially along altered zones (Dardier *et al.,* 2001; Dardier, 2004).

The investigated areais structurally controlled by NW-SE trending (Gulf of Suez) trend and N-S. The aim of the present work deals with the granitic rocks at El-Gidami area. Field trips had been done and the area under investigation was mapped using aerial photographs. More than 80 rock samples were collected from the different exposed rock units, and 35 of rock samples were subjected to petrographical studies. Some selected samples representative (20) were subjected to the chemical analyses in the Acme Lab in Canada, for major oxides, trace elements and REE.

2- Geologic Settings

El Gidami area lies between Latitudes 26° 20' and 26° 28' N. and Longitudes 33° 21' and 33°29'E, Central Eastern Desert of Egypt, at kilometer 85 Qena – Safaga road. El Gidami area is composed of amphibolite rocks, older granites (OG) and younger granites (YG). The older rock unitexposed in the study area is amphibolite rocks, which forms a narrow hills of low heights and outcropped the eastern part of the study area (Fig.1). It is usually hard and massive with moderate resistance to erosion.

The older granites (OG) are intruded by younger granites that have a gradational to sharp contact with the other rocks. They occurred in the south western and the eastern parts of the study area. They are easily weathered, eroded and form low terrains and characterized by whitish grey to dark grey colors. The

older granites are medium to coarse-grained, exfoliated; so it is difficult to get a fresh rock sample.

Younger granites (YG) represent the most dominant rock units in the investigated area and intrude into amphibolite and older granites and showing gradational to sharp contact. This sharp contact indicates passive epizonal emplacement. They possess the highest level of normal gamma radioactivity among all the other rocks. They varies from medium to coarse-grained rocks with pink to reddish in color. They form the most topographic features with oval, rounded outline and form the highest peaks in the area. They show cavernous weathering with different size, vertical jointing and exfoliation and enriched with xenoliths of pre-existing rocks.

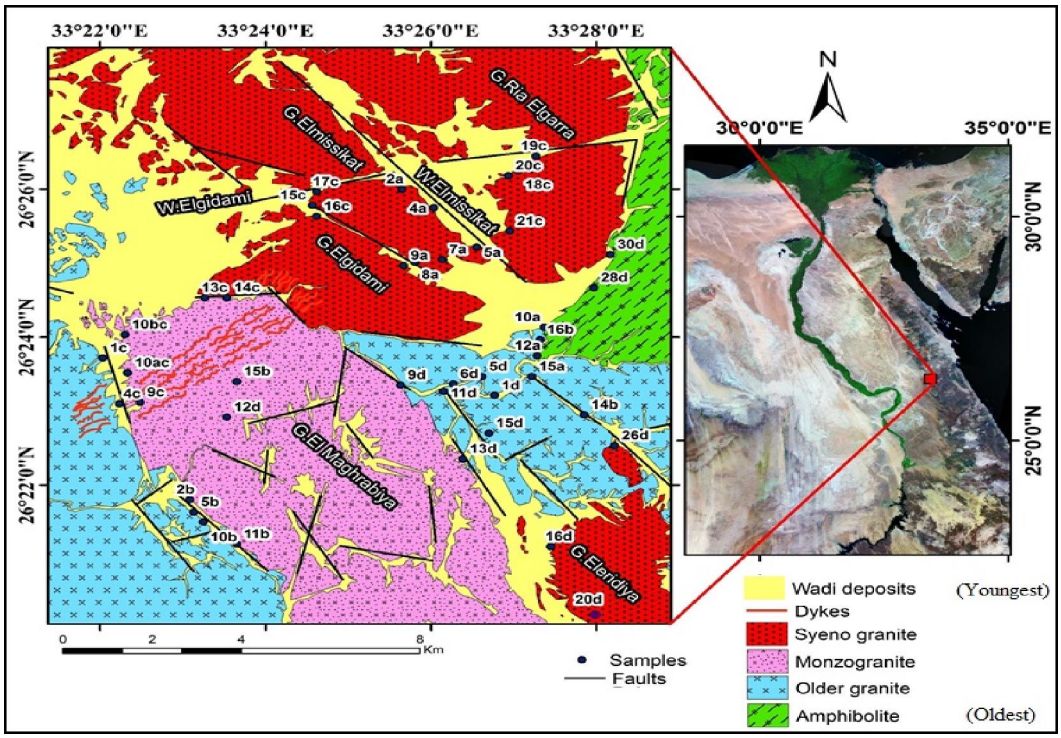

Fig.1: Geologic map of the studied area including samples location.

3-Petrography

Petrographical studies of the different rock unites of El-Gidami area, were carried out for nomenclature and proper identification of essential and accessory minerals as well as the texture of the studied rocks. According to the modal composition of the studied granitic rocks plotted in IUGS diagram, the older granites are represented by tonalite and granodiorite whereas the younger granites are represented by monzogranite and syenogranite (Table 1.1) (Fig.2).

Amphiobolites are composed mainly of tremolite, actinolite, hornblende, plagioclase, few quartz grainsand few minute iron oxides as accessories. Tremolite and actinoliteare very irregular, exhibits brownish green color. They are represented by laths or large crystals, varying in size and shape and altered to chlorite (Fig.3.A). Hornblende exhibiting two set of cleavage and mostly enclosed with tremolite and actinolite (Fig.3.B).

Older granite are medium to coarse grained and composed of plagioclase, quartz, potash feldspars, hornblende and biotite as essential minerals. Zircon and opaquescrystals are present as accessory minerals, while epidote and sericite are secondary minerals. Plagioclaseoccurs as prismatic euhedral to subhedral crystals. They are altered to saussurite and epidote minerals especially along their peripheries (Figs. 3. C & D). Potash feldsparoccurs as orthoclase perthite, which shows dusty surface due to alteration. Hornblendeoccurs as anhedral to subhedral and is partially altered to chlorite. Biotiteoccurs as flake crystals with brown colors and is commonly altered to pale green chlorite (Fig.3.E). Quartz shows undulose extinction and are highly cracked, indicating that they are subjected to stresses. Zircon is found in minor amount, as a short minute prismatic crystals included within plagioclase crystals.

The younger granites in the study area are classified into two types; monzogranite and syenogranite according to Q-A-P Streckeisen (1976) diagram. There is a similarity in petrographic description of the two types but they differ in the

percentage of felsic minerals, where monzogranite consists mainly of quartz, plagioclase, potash feldspar (perthite), biotite and few amounts of muscovite as essential minerals, while syenogranite is composed of quartz, potash feldspars, plagioclase, muscovite and a few amount of biotite as essential minerals. Zircon, sphene andiron oxides are accessory minerals, whereas sericite, epidote and clay are secondary minerals.

Potash feldspars arerepresented by orthoclase perthite which occurs as weather flamy, stringy or veinlet perthite (Fig.3.F). Orthoclase perthite occurs as subhedral to anhedral prismatic crystals. They show intergrowth with quartz to give micrographic texture. Plagioclase occurs as euhedral to subhedral crystals and altered to saussourite and epidote where their cores are usually more altered than the outer rims. The reaction rim of albite formed between two crystals of perthite (Fig.4.A). Plagioclase crystals are twisted and dislocated due to stress (Figs.3.B & C). Quartz shows normal and undulose extinction and has a variable sizes and shapes and sometimes occur as skeleton or veinlet in plagioclase (Figs.4.D & E). Muscoviteis represented by fine grains, usually filling the fracture of perthite. Biotite occurs as yellowish brown sub-hedral flaky crystals yielding patches of green color (chlorite) particularly along cleavage and cracks. Some of these biotite crystalsare enriched with iron oxides and sometime contain crystals of allanite (Fig.4.F).

Table 1: Modal composition of El-Gidami granitic rocks.

S.N.	Quartz	Plagioclase	K-feldspar	Biotite	Muscovite	Hornblende	Accessories	Iron-oxide	Total
	Tonalite								
15A	45.00	44.00	2.80	1.20	-	0.50	4.00	2.50	100%
20A	55.00	42.00	1.00	1.00	-	0.20	1.60	0.20	100%
14B	33.00	55.00	3.00	1.00	0.20	2.80	4.00	1.00	100%
15B	23.00	71.00	0.80	0.2	-	1.50	2.50	1.00	100%
16B	35.00	62.00	-	1.00	-	1.00	1.00	-	100%
5D	24.00	62.00	2.00	3.60	0.40	4.00	3.05	1.00	100%
6D	27.40	63.40	-	3.10	-	-	2.70	1.60	100%
11D	52.00	44.00	0.50	1.60	-	-	1.00	0.90	100%
24D	27.00	62.00	3.00	3.80	-	-	2.90	1.30	100%
	Granodiorite								
6B	20.00	60.40	12.00	5.00	1.00	-	0.60	1.00	100%
10B	25.00	64.00	4.5	3.60	0.40	-	0.5	2.00	100%
1C	29.00	47.00	16.00	4.65	0.56	-	0.89	1.800	100%
	Monzogranite								
2B	30.00	38.50	25.30	2.80	1.20	-	0.60	1.60	100%
7D	40.00	29.00	30.00	0.50	-	-	-	0.50	100%
10D	38.00	36.30	23.30	1.10	0.20	-	0.40	0.70	100%
13D	24.60	41.40	32.40	1.00	0.60	-	-	-	100%
11B	28.40	36.30	33.70	-	0.2	-	1.40	-	100%
31D	35.00	39.00	23.00	1.20	0.20	-	0.30	1.30	100%
10C	31.00	41.50	26.00	0.80	-	-	0.70	-	100%
14C	31.40	24.50	41.30	2.00	0.50	-	0.20	0.10	100%
17D	38.00	34.00	25.00	1.40	0.30	-	0.30	1.00	100%
20C	26.00	41.00	30.00	2.20	-	-	0.30	0.50	100%
	Syenogranite								
1A	30.50	19.30	44.00	3.80	0.30	-	0.03	2.07	100%
8A	42.00	12.00	42.60	2.2	0.80	-	-	0.40	100%
9A	26.00	23.00	48.00	1.1	-	-	0.6	-	100%
16C	24.00	21.00	54.00	1.2	0.10	-	-	-	100%
17C	26.00	22.00	50.00	1.5	0.60	-	-	0.40	100%
18C	42..40	18.00	38.00	0.50	-	-	0.40	0.70	100%
4A	32.00	20.60	46.40	0.70	-	-	-	0.30	100%
21C	35.00	20.00	44.20	-	0.20	-	0.40	-	100%
26D	48.00	7.80	43.00	0.40	0.5	-	-	0.80	100%
30D	30.20	18.00	45.00	1.10	3.00	-	0.50	2.20	100%
16D	34.30	22.00	43.24	0.14	0.11	-	0.11	0.10	100%

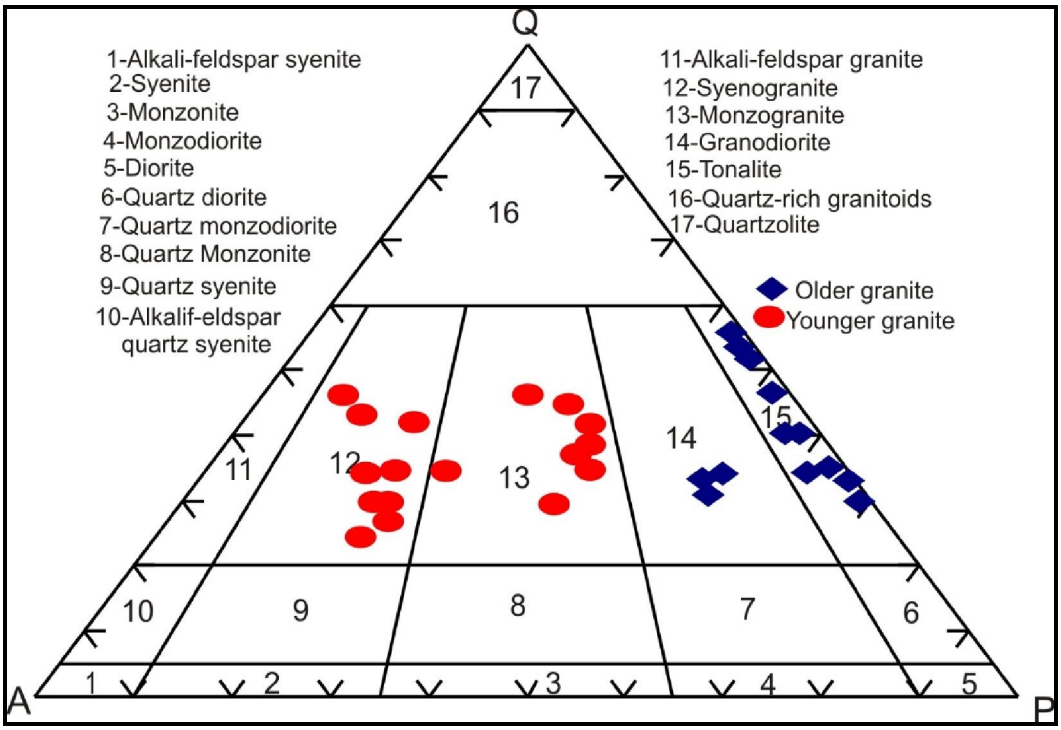

Fig.2: IUGS classification ofEl-Gidami granitic rocks plotted on QAP ofStreckeisen diagram (1976), where Q=Quartz, A=Alkali feldspars and P=Plagioclase.

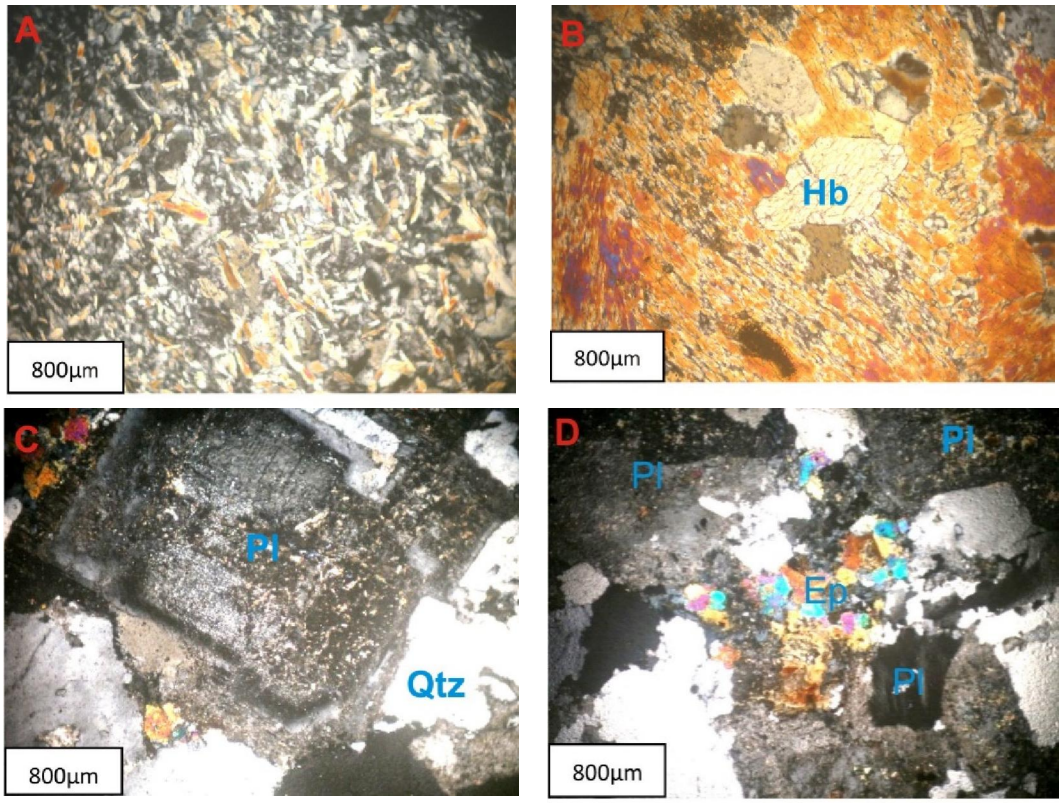

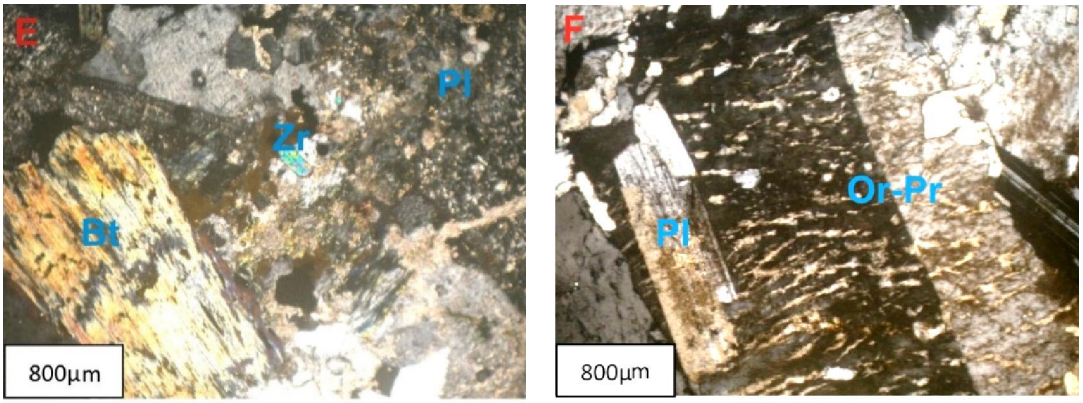

(Fig.3) Notes, Symbols of rock-forming minerals after **Kretz, R. (1983).**
The following photomicrographs showing the:
A: Laths of tremolite and actinolite crystals (amphibolite); C.N.
B: Hornblendecorroborated byactinolte (amphibolite); C.N.
C: Crystals of highly altered of plagioclase (older granite); C.N.
D: Well developedcrystals of epidote on the periphery of plagioclase (older granite); C.N.
E: Partially altered biotite to chlorite and crystal of zircon in plagioclase (older granite); C.N.
F: Veinlet orthoclase perthite crystals enclosing an altered plagioclase crystal(younger granite); C.N.

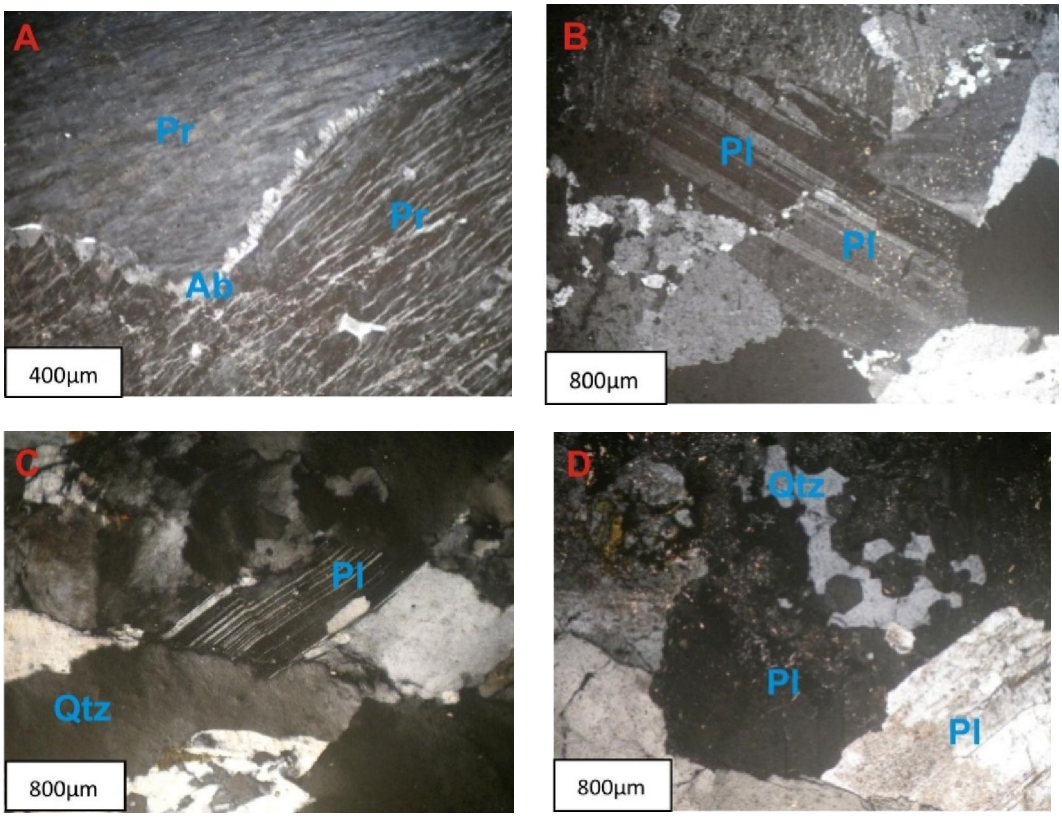

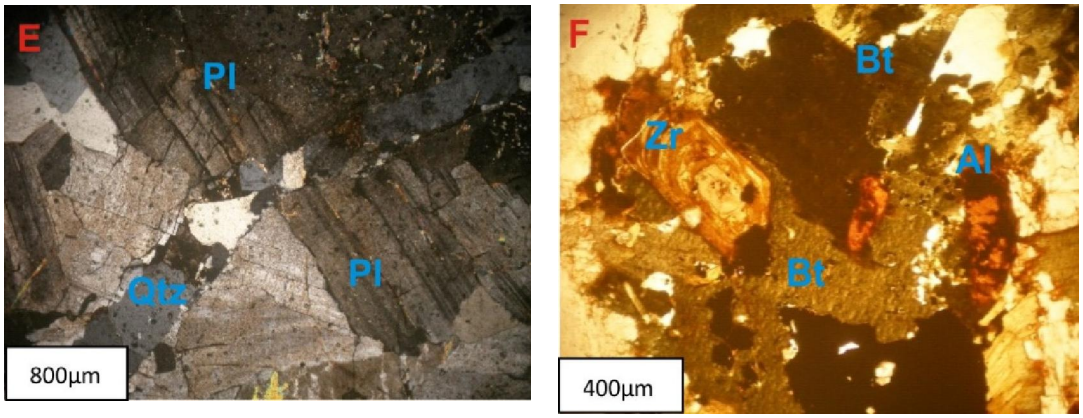

(Fig.4) The following photomicrographs showing the:

A: Reaction rim of albite between two crystals of perthite (younger granite); C.N.
B: Dislocation of plagioclase due to the deformation (younger granite); C.N.
C- Twisting of plagioclase (younger granite); C.N.
D- Plagioclaseencloses skeleton of quartz crystals (younger granite); C.N.
E- Veinlet of quartz in plagioclase (younger granite); C.N.
F: Zircon and allanite crystals embedded in biotite (younger granite); P.P.

Table 2: Major oxides (wt %) of El-Gidami granitic rocks.

	Older granite								Younger granite																
	Tonalite					Granodiorite			Monzogranite								Syenogranite								
S. No.	5D	11D	14A	14B	Av.	6B	10B	Av.	20C	11B	14C	13D	7D	10C	Av.	1A	9A	17C	18C	26D	30D	4A	16C	Av.
SiO_2	67.5	71.5	72.6	70.5	70.5	65.1	64.2	64.6	73.5	75.1	73.2	74.3	76.2	75.7	74.6	75.8	76.77	75.6	76.6	75.3	73.9	75.1	76.8	75.7
TiO_2	0.33	0.24	0.24	0.27	0.27	0.50	0.51	0.51	0.16	0.08	0.15	0.09	0.09	0.10	0.11	0.07	0.07	0.08	0.07	0.00	0.1	0.05	0.05	0.06
Al_2O_3	15.	13.7	13.6	13.7	14.0	16.0	16.3	16.2	13.3	12.8	13.5	13.4	12.2	12.6	12.9	12.0	11.8	12.5	12.3	13.0	13.3	12.2	12.5	12.4
Fe_2O_3	3.52	2.77	2.22	3.20	2.9	3.00	3.02	3.01	1.39	0.71	0.99	0.76	0.63	0.77	0.8	1.14	1.02	1.17	0.61	0.56	1.2	0.99	0.59	0.91
FeO	3.16	2.50	1.99	2.88	2.6	2.70	2.71	2.7	1.25	0.64	0.89	0.68	0.57	0.69	0.78	1.03	0.91	1.05	0.55	0.5	1.08	0.89	0.53	0.82
MnO	0.05	0.03	0.04	0.07	0.04	0.06	0.06	0.06	0.03	0.09	0.07	0.05	0.04	0.04	0.05	0.02	0.02	0.03	0	0.02	0.03	0.02	0.01	0.02
MgO	0.93	0.81	0.60	0.76	0.77	1.13	1.08	1.1	0.17	0.07	0.23	0.18	0.13	0.13	0.15	0.03	0.05	0.05	0.03	0.03	0.07	0.05	0.03	0.04
CaO	4.66	2.80	2.70	2.91	3.26	2.53	2.50	2.5	0.73	0.55	0.64	0.56	0.50	0.36	0.56	0.52	0.35	0.49	0.5	0.1	0.62	0.53	0.48	0.45
Na_2O	3.86	3.91	4.60	4.26	4.1	5.06	5.11	5.1	4.11	4.62	5.34	4.8	4.6	4.69	4.69	4.33	4.09	4.21	3.94	4.46	4	4.41	4.04	4.2
K_2O	0.19	0.83	0.48	0.51	0.50	3.13	3.40	3.3	4.95	4.53	4.48	4.55	4.58	4.23	4.5	4.29	4.58	4.52	4.84	5.78	5.12	4.99	4.51	4.8
P_2O_5	0.05	0.03	0.03	0.03	0.35	0.14	0.15	0.14	0.03	0.03	0.05	0.03	0.03	0.02	0.03	0.001	0.001	0.002	0.001	0.001	0.01	0.001	0.001	0.002
L.O.I	0.37	0.79	0.80	0.82	0.69	0.56	0.40	0.48	0.27	0.70	0.37	0.55	0.3	0.6	0.46	0.65	0.34	0.32	0.44	0.29	0.5	0.32	0.37	0.41
Fe_2O_3/MgO	3.78	3.42	3.70	4.2	3.77	2.65	2.79	2.7	8.17	10.1	4.3	4.2	4.8	5.92	6.3	38	20.40	23.4	20.3	28	17.1	19.8	19.6	23.3
Na_2O/K_2O	20.3	4.7	9.5	8.35	10.7	1.62	1.63	1.6	0.83	1.02	1.21	1.05	1.00	1.11	1.03	1.00	0.89	0.93	0.81	0.77	0.78	0.88	0.89	0.86
ASI	1.76	1.82	1.76	1.78	1.78	1.49	1.48	1.4	1.37	1.32	1.29	1.35	1.26	1.36	1.3	1.31	1.30	1.35	1.33	1.25	1.3	1.23	1.33	1.3
DIF. index	66	76	79	75	74.0	78	80	79	93	96	95	96	96	97	95	96	97	95	97	98	94	95	96	96

Table 3: Trace elements (ppm) of the studied granitic rocks.

	Older granite						Younger granite													
	Tonalite				Granodiorite		Monzogranite						Syenogranite							
S. No	5D	11D	14A	14B	6B	10B	20C	11B	14C	13D	7D	10C	1A	9A	17C	18C	26D	30D	4A	16C
Sr	116.0	131.0	93.00	118.0	527.0	555.0	70.00	63.00	114.0	76.00	60.00	65.00	12.00	9.00	14.00	14.00	3.00	34.00	10.00	13.00
Ga	13.92	10.93	12.98	12.91	21.94	21.04	23.16	19.64	21.74	21.59	19.84	19.89	28.05	25.92	28.64	29.62	62.91	25.76	31.05	27.97
Ba	111.0	215.0	210.0	170.0	712.0	702.0	263.0	726.0	1016	861.0	660.0	767.0	58.00	35.00	72.00	53.00	43.00	182.0	52.00	47.00
Cs	0.30	0.70	0.40	0.30	1.10	1.90	2.4	1.3	1.6	1.8	1.7	0.8	3.2	2.2	2.3	2	2.00	9.3	2.3	1.5
Tl	0.05	0.1	0.08	0.06	0.35	0.37	0.97	0.47	0.52	0.45	0.57	0.46	1.09	1.08	1.09	1.16	2.33	1.52	1.38	1.23
Rb	4.80	23.50	13.30	7.90	61.00	67.20	177.8	88.1	85.7	83	101.3	75.8	199	211.5	197.3	194	548.7	316	255.2	247.1
Li	7.40	9.10	6.70	8.70	13.50	25.80	32.4	6.6	15.6	12	31.7	4.6	67.3	57.5	56.7	3.3	45.8	115.3	55.8	7.80
Zr	64.30	51.20	64	49.6	52.00	62.1	140.8	69.7	72.6	63.1	72.1	74.1	131	115.1	126.4	155.6	240.7	114.9	123.1	131.3
Nb	1.75	1.60	3.20	1.86	9.77	10.60	28.04	20.75	20.94	20.94	26.8	23.04	48.02	53.18	43.86	46.57	57.15	39.44	38.41	63.94
Hf	2.06	1.82	2.26	1.62	2.02	2.66	5.12	2.86	2.95	2.85	3.18	3.18	6.08	4.77	5.43	6.82	20.91	4.96	6.62	6.32
Cr	12.00	13.00	9.00	9.00	16.00	13.00	11.00	4.00	5.00	4.00	3.00	3.00	6.00	4.00	3.00	5.00	4.00	5.00	4.00	4.00
Ni	1.70	2.50	1.20	1.20	7.90	8.30	1.2	0.6	2.4	1.6	1.3	1.4	1.00	1.00	1.40	0.80	0.80	1.30	0.70	1.50
V	49.00	38.00	24.00	28.00	37.00	36.00	6.00	3.00	5.00	3.00	2.00	3.00	1.00	1.00	1.00	1.00	1.00	1.00	1.00	1.00
Zn	16.90	12.60	22.00	52.70	63.50	58.6	40.1	39.6	42.6	62.5	54.1	61	66.8	66.4	58.8	41.2	698.8	69.7	50.1	145.6
Co	7.50	5.10	3.70	5.00	6.20	6.90	1.1	0.4	1.00	0.6	0.4	1.1	0.3	0.2	0.4	0.2	0.2	0.5	0.2	0.2
Cu	2.12	1.85	5.41	13.34	4.22	3.01	1.55	2.29	0.95	0.71	1.08	4.42	0.66	1.13	1.47	1.6	0.8	1.23	1.2	5.91
Y	24.80	19.40	28.30	18.70	15.40	15.8	55.3	14.8	15.9	13.2	7.4	12.1	83.9	80.4	71.9	85	49	57.4	98.7	96.2
U	0.40	0.70	2.30	0.50	2.10	3.20	7.3	2.1	1.9	3	1.4	1.6	9	9.8	10.8	11.3	4	7.6	11.1	11.8
Th	0.80	0.70	1.10	0.30	6.90	7.10	18.6	5.7	5.8	7.2	5.9	5.8	28.5	26.9	30	23.8	16.1	17.5	24.3	32.1
Ba/Sr	0.95	1.64	2.26	1.44	1.35	1.26	3.75	11.52	8.91	11.33	11	11.8	4.83	3.89	5.14	3.78	14.30	5.35	5.20	3.62
Rb/Sr	0.04	0.18	0.14	0.07	0.12	0.12	2.54	1.39	0.75	1.09	1.68	1.17	16.58	23.50	14.09	13.85	182.9	9.92	25.52	19.00

Table 4: The CIPW norm of the studied granitic rocks.

	Older granite						Younger granite													
Norm	Tonalite				Granodiorite		Monzogranite						Syenogranite							
	5D	11D	14A	14B	6B	10B	20C	11B	14C	13D	7D	10C	1A	9A	17C	18C	26D	30D	4A	16C
Qz	32.13	37.97	37.09	36.02	16.33	15.93	28.63	30.05	23.94	27.78	31.64	31.51	33.35	34.76	32.55	34.27	29.63	29.47	29.81	35.04
Or	1.13	4.95	2.86	3.03	18.62	20.50	29.36	26.98	26.60	27.06	27.06	25.17	25.54	27.18	26.8	28.75	30.57	30.44	29.76	26.77
An	22.92	13.84	13.33	14.32	11.75	11.75	3.41	0.89	00.00	1.55	00.00	0.89	0.77	0.28	1.86	1.71	0.32	3.03	00.00	2.33
Ab	32.74	33.33	39.19	36.14	43.02	44.02	34.83	26.98	44.80	40.79	37.47	39.88	36.83	34.68	35.68	33.44	38.04	33.98	35.35	34.27
Di	00.00	00.00	00.00	00.00	00.00	00.00	0.04	1.45	2.42	0.89	1.96	0.67	1.56	1.23	0.46	0.63	0.11	00.00	2.28	00.00
Hy	4.78	4.02	3.02	3.50	4.61	1.98	1.34	0.06	0.19	0.58	0.12	0.53	0.13	0.24	0.77	0.16	0.47	1.06	0.26	0.50
Ilm	0.63	0.46	0.46	1.37	0.96	0.99	00.30	0.15	0.29	0.17	0.17	0.19	0.13	0.13	0.15	0.13	0.02	0.19	0.10	0.10
Ap	0.11	0.07	0.07	0.07	0.33	0.33	00.07	0.07	0.11	0.07	0.07	0.04	0.02	0.02	0.02	0.02	0.02	0.02	0.02	0.02
Crn	0.44	1.31	0.73	0.91	00.00	0.02	00.00	00.00	00.00	00.00	00.00	00.00	00.00	00.00	00.00	00.00	00.0	0.03	00.00	0.02

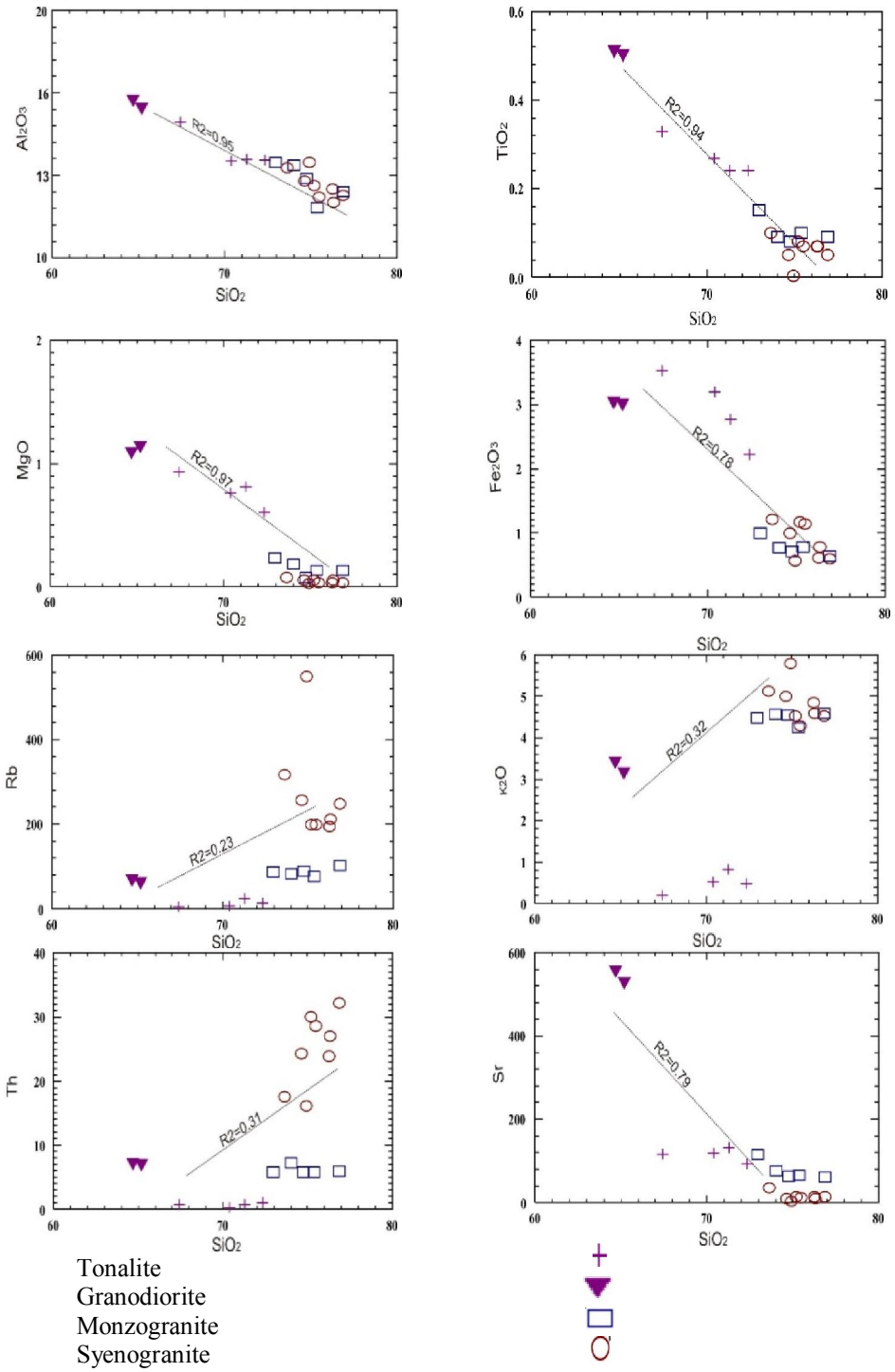

Fig. 5: Plotting of some major oxides and trace element versus SiO_2.

3-Geochemistry

Chemical analyses of the whole-rock representative samples (20) were carried out at ACME analytical Laboratories of Vandcouver, Canada. These samples were chemically analyzed for major oxides, trace and rare earth elements.

3.1-Major oxides and trace element

The results of complete analysis for the major oxides and some trace elements of the studied granitic samples are given in the (Tables 2, 3 respectively) and the CIPW norm were calculated and given in the (Tables 4). The studied tonalite rocks show high silica content with an average (70.57), while the granodiorite show intermediate silica values with an

average (64.69). On the other hand, monzogranite and syenogranite show high silica content with an average (74.40 & 75.70 respectively).The narrow range in the SiO_2 values indicates homogeneity of the studied granitic masses.

Harkervariation diagrams are used in this study to show the relationship between distribution of SiO_2 values of the granitic rocks against major oxides and some trace elements. There is a negative correlation between TiO_2, Al_2O_3, $Fe_2O_3$and MgO) where these oxides decrease with increasing SiO_2); while K_2O and Na_2O show a positive correlation. In addition, some trace elements are plotted against SiO_2. The Rb, and Th show a positive correlation from tonalite to syenogranite, while Sr shows a negative correlation (Fig.5).

The geochemical classification of the studied granitic rocks is depicted from SiO_2 versus (Na_2O+K_2O) variation diagram by Middlemost (1985) (Fig.6). This diagram shows that, tonalite samples plot in the tonalite field, granodiorite plot in the granodiorite fields and the younger granites plot in the granite field. Plotting the examined granitic rocks in ternary normative Or-Ab-An diagram of O'Connor (1965) and modified by Barker (1979) (Fig.7) gives the same results. Plotting the examined granitic rocks in ternary normative Ab-An-Or diagram of Streckeisen (1976), the syenogranite and monzogranite samples plot in the alkali graniteand syenogranite due to the enrichment of SiO_2, granodiorite samples fall in the boundary between the monzogranite and granodiorite fields. The tonalite samples plot in the tonalite field (Fig.8).

According to SiO_2 versus (Na_2O+K_2O) diagram suggested by Iverine and Baragar (1971), to distinguish between the alkaline and sub-alkaline nature of magma, the plotted samples have sub-alkaline affinity (Fig.9). Based on Fe_2O_3+FeO versus Al_2O_3 binary diagram that suggested by Abdel-Rahman (1994) to distinguish between the alkaline, peraluminous and calc-alkaline magmatic nature, the studied granitic samples plotted in the peraluminous and calc-alkaline fields (Fig.10). SiO_2 versus Zr binary diagrams of Günther *et al.,* (1989), all samples of tonalite, granodiorite and monzogranite plotted on the field of I-type granitites. Meanwhile all samples of syenogranite fall in A-type granites (Fig.11).

Pearce *et al.,* (1984) proposed the log Y-Nb binary diagrams to differentiate between the different tectonic settings of the granitic rocks. The older granite and monzogranite plotted in the field of volcanic arc granite, while the syenogranite falls in the field of within plate granite (Fig.12). Condie (1973) proposed the Sr versus Rb binary diagram to differentiate the petrogenesis of the studied granitic rocks. Tonalite formed in the lower crust (15-20 km) due to depletion in Rb, meanwhile granodiorite, monzogranite and syenogranite come from the upper mantle (20-30km, Fig.13).

3.2-Ree

Geochemistry

The rare earth elements (REEs) are a useful geochemical tool where they could give valuable information about rock genesis. The REEs comprise the lanthanides group, which includes 14 elements from lanthanum (La) to lutetium)Lu).Taylor and Mclennan (1985) considered that the REEs in the upper crust are richer than the lower crust. The lanthanides are known by their very similar chemical and physical properties. They (as well as U and Th) behave incompatibly during magmatic processes. However, crystallization of small amounts of accessory minerals (of larger cation sites) such as zircon, garnet, monazite, allanite, xenotime, apatite and sphene, would control the REEs contents during crystallization of the magma and might lead to depletion of REEs in the residual fluids (Henderson, 1996).

The total REE contents of the studied granitic rocks aregiven in (Table 4), with an average for tonalite, granodiorites, monzogranites and syenogranites 37.84×10^{-6}, 112.42×10^{-6}, 78.45×10^{-6} and 174.23×10^{-6} respectively which indicates that these granites are depleted in REE according to Hermann, (1970), ($250–270\times10^{-6}$).

The chondrite- normalized REE patterns of the studied granodiorite and monzogranites show well-fractionated patterns $(La/Yb)_N$ = (7.85 and 4.1) and slightly in tonalite and syenogranite (1.02 and 1.4) respectively. The LREEs of tonalite and syenogranite show slightly fractionated (La/Sm=0.97& 1.1) and well-fractionated in granodiorite and monzogranite (La/Sm=3.1 &2.1).The fractionation of HREE of the studied tonalite, granodiorite, monzogranite and syenogranite rocks are very slightly (Gd/Yb=0.97, 1.5, 1.3 & 0.83 respectively). Granodiorite, tonalite, monzogranites and syenogranites REE diagram show a positive Ce anomalies indicates low O fugacity at the source of the magma (Constantopoulos, 1988).

Chondrite-normalized REE diagram (Boynton, 1984) of tonalites, monzogranites and syenogranites show a negative correlation with Eu, while granodiorite have positive correlation with Eu (Figs.14, 15, 16&17), positive correlation may be due to the high value of Sr content, So the Eu is substituted by Sr cations. this lead to the change of Eu/Eu* anomaly value for this granite variety. Negative Eu resulted from plagioclase feldspar fractionation, together with the low Sr content (103 ppm on average). The principal carriers of REEs in most granites are the accessory minerals such as monazite, zircon, apatite, xenotime and titanite in

addition to plagioclase in the case of Eu (Gromet and Silver, 1983, Saleh *et al.,* 2002 and Moghazi *et al.,* 2004), therefore, fractionation of accessory minerals would result in a lowering of REEs content.

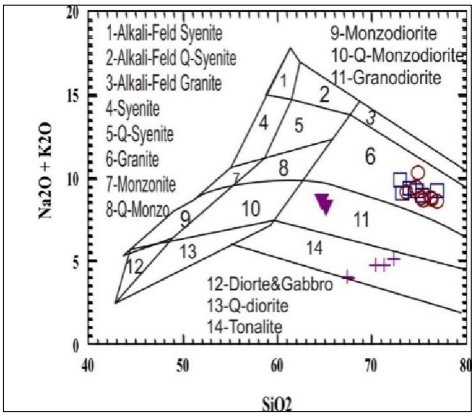

Fig.6: SiO2 vs. (Na2O+K2O) variation diagram of Middlemost (1985) for the studied granitic rocks. Symbols as in Fig.4.

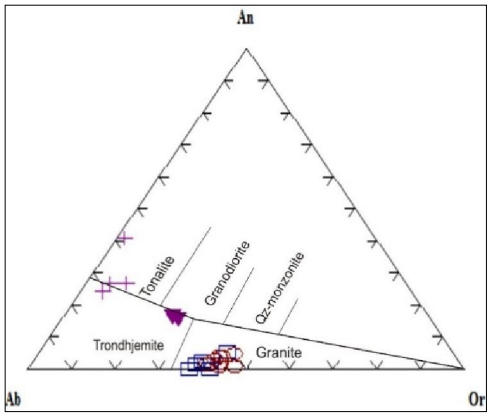

Fig.7: Ab-Or-An ternary diagram, for the granitic rocks after O'Connor (1965) and modified by Barker (1979). Symbols as in Fig.4.

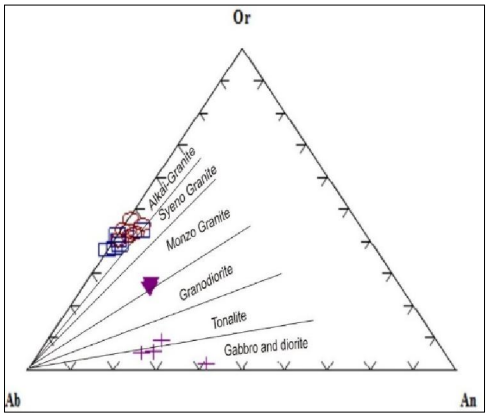

Fig.8: Ab–Or–An ternary Diagram, for the granitic rocks after Streckeisen(1976). Symbols as in Fig.4.

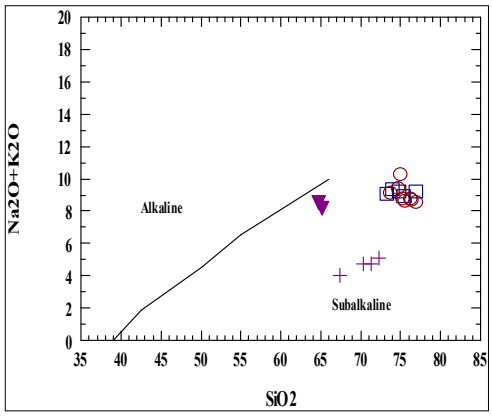

Fig.9:TAS diagram of Irvine and Baragar (1971) for the granitic rocks. Symbols as in Fig.4.

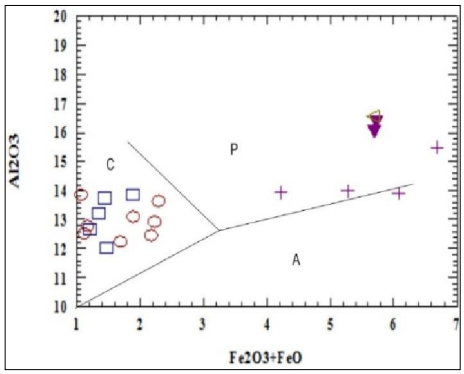

Fig.10: Fe_2O_3+FeO - Al_2O_3 diagram of Abdel-Rahman (1994) for the granitic rocks (A-Alkaline, P-Peraluminous and C-Calc-alkaline). Symbols as in Fig.4.

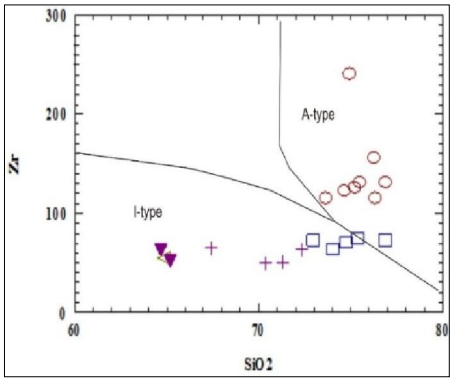

Fig.11: SiO_2 versus Zr binary diagram of Günther *et al.,* (1989) for the examined granitic rocks. Symbols as in Fig.4.

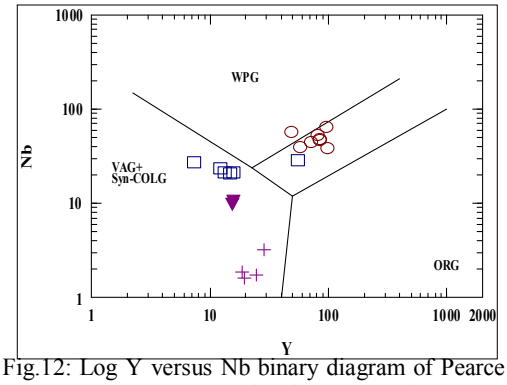

Fig.12: Log Y versus Nb binary diagram of Pearce *et al.,* (1984). VAG= Volcanic Arc Granites, Syn-COLG=Syn-collision granites, WPG= Within Plate Granites, ORG = Ocean Ridge Granites. Symbols as in Fig.4.

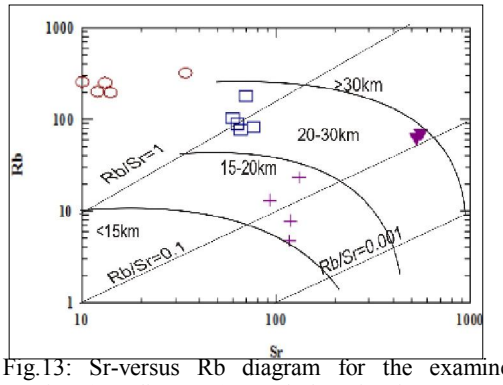

Fig.13: Sr-versus Rb diagram for the examined granites (Condie, 1973). Symbols as in Fig.4.

4: Fractional modelling and mass balance:

In order to constrain the fractional crystallization hypothesis quantitatively, the linear least-squares mass-balance method given by Wright and Doherty(1970) were applied. The computation program calculates the relative proportion of the fractioning liquid minerals (phases) and the amount of the residual liquid required to match the composition of the parent, whereas the rock with the lowest SiO_2 content can be assumed the parent rock (PR), a sample with a higher SiO_2 content is considered the daughter rock (DR). To test the hypothesis, a mass balance calculation could be performed, knowing the compositions of the parent and the daughter rocks and their respective modal minerals. The compositions of the fractioned phases are chosen from Deer *et al.,*(1966) with the guidance of the normative studies. The method tries to minimize sum square of the residuals ($\sum R^2$). The smaller value of the ($\sum R^2$) indicates a good fit of the resulting model. The calculation has been performed for the granodiorite and the younger granite (monzogranite) of Gabal El-Gidami as one separate system, then granodiorite and the younger granite (syenogranite) of Gabal El-Gidami as another separate system.

Within the granodiorite and younger granite (monzogranite) system, the observed daughter or the most compositionally evolved younger granite sample (S.No.7D, Table 2), can be derived from the most mafic magma of the observed parent granodiorite sample (S.No.10B, Table2) by fractional crystallization of plagioclase 13.39%, hornblende 3.60%, biotite 15.23%, orthoclase 43.51%, quartz 11.80% and apatite 0.43 % with 12.04% residual liquid sample (S.No. 7D). The relatively small valueof $\sum R^2$ (0.006) indicates a good fit of the resulting model. The results are tabulated in (Table 6).

Within the granodiorite and younger granite (syenogranite) system, the observed daughter or the most compositionally evolved younger granite sample (S.No.16C, Table 2), can be derived from the most mafic magma of the observed parent granodiorite sample (S. No. 10B, Table 2) by fractional crystallization of plagioclase 11.94%, hornblende 3.69%, biotite 15.25%, orthoclase 46.01%, quartz 11.87% and apatite 0.52 % with 10.72% residual liquid sample (S.No. 16C). The relatively small value of $\sum R^2$ (0.007) indicates a good fit of the resulting model.The results are tabulated in (Table 7).

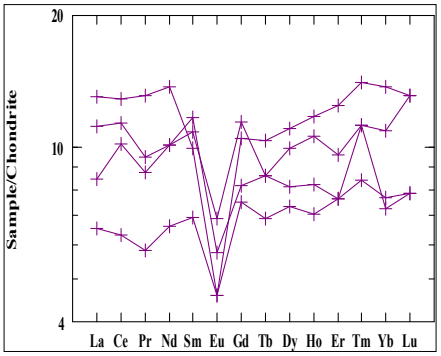

Fig.15: Chondrite-normalized REE diagram Boynton (1984) for the investigated tonalites.

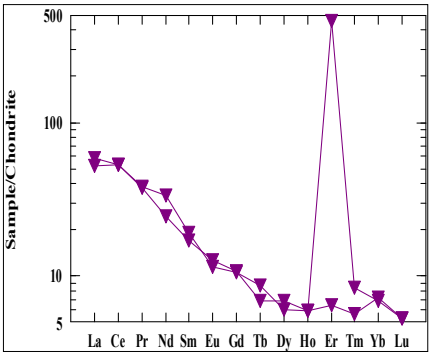

Fig.16: Chondrite-normalized REE diagram Boynton (1984) for the investigated granodiorites.

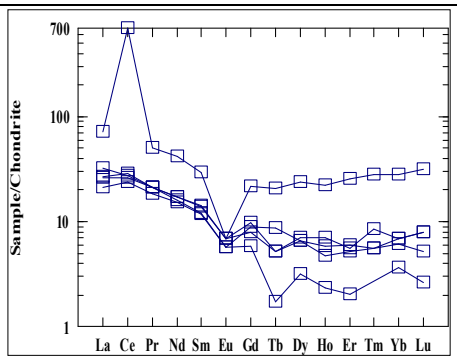

Fig.17: Chondrite-normalized REE diagram Boynton (1984) for the investigated monzogranites.

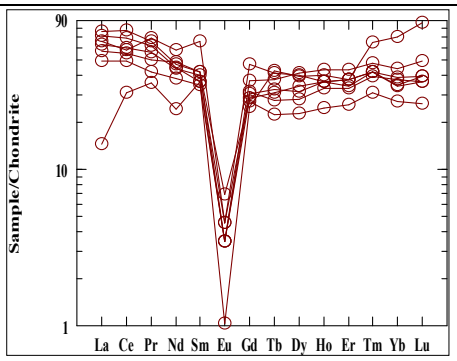

Fig.18: Chondrite-normalized REE diagram Boynton (1984) for the investigated syenogranites.

Table 5: The REE of the studied granitic rocks.

Elements	Older granite						Younger granite												
	Tonalite				Granodiorite		Monzogranite						Syenogranite						
	5D	11D	14A	14B	6B	10B	20C	11B	14C	13D	7D	10C	1A	9A	17C	18C	26D	30D	4A	16C
La	4.10	2.40	4.80	3.10	19.20	21.50	26.4	9.50	11.9	9.90	7.70	8.00	23.2	18.3	26.2	24.2	5.3	28.1	17.5	21.1
Ce	10.89	6.05	12.37	9.77	50.40	50.94	65.41	24.84	26.55	27.22	22.97	28.20	57.7	47.58	66.45	55.57	<0.1	74.08	0.30	0.30
Pr	1.30	0.80	1.80	1.20	5.20	5.10	6.90	2.90	2.90	2.90	2.50	2.80	7.70	5.80	8.50	9.50	29.55	9.10	49.09	53.08
Nd	7.20	4.70	9.80	7.20	23.90	17.40	30.0	12.30	12.30	11.50	10.80	10.80	31.3	27.20	31.80	41.3	4.90	33.4	6.40	6.90
Sm	2.50	1.60	2.30	2.70	4.40	3.90	6.80	3.20	3.30	2.80	2.70	3.00	9.30	8.00	8.40	15.3	17.30	9.70	27.3	34.4
Eu	0.60	0.40	0.40	0.50	1.00	1.10	0.60	0.60	0.60	0.50	0.50	0.40	0.40	0.30	0.30	0.40	8.40	0.60	10.50	9.80
Gd	3.50	2.30	3.20	2.50	3.20	3.30	6.70	3.00	2.40	2.70	1.80	2.40	9.30	8.70	9.70	14.5	7.70	8.40	11.6	11.3
Tb	0.50	0.40	0.60	0.50	0.50	0.40	1.20	0.30	0.30	0.50	0.10	0.30	1.90	1.80	1.60	2.40	2.50	1.30	1.90	2.20
Dy	3.80	2.80	4.20	3.10	2.30	2.60	9.10	2.50	2.70	2.50	1.20	2.10	12.1	13.10	10.70	15.20	15.10	8.70	14.4	15.90
Ho	0.90	0.60	1.00	0.70	0.50	0.50	1.90	0.50	0.60	0.40	0.20	0.40	3.10	3.10	2.80	3.10	3.40	2.10	3.40	3.70
Er	2.40	1.90	3.10	1.90	1.60	1.50	6.10	1.50	1.40	1.30	0.50	1.20	8.50	9.40	8.30	9.30	9.40	6.50	10.6	10.80
Tm	0.40	0.30	0.50	0.40	0.20	0.30	1.00	0.20	0.30	0.20	0.08	0.20	1.50	1.50	1.40	1.50	2.30	1.10	1.90	1.70
Yb	2.70	1.90	3.40	1.80	1.80	1.70	6.90	1.70	1.70	1.50	0.90	1.50	8.50	8.60	9.30	9.70	17.50	6.80	14.10	10.90
Lu	0.50	0.30	0.50	0.30	0.20	0.20	1.20	0.30	0.30	0.20	0.10	0.20	1.40	1.50	1.40	1.50	3.30	1.00	2.20	1.90
T.REE	41.3	26.45	47.97	35.67	114.4	110.4	169.9	63.34	67.25	64.12	51.97	54.13	175	154.8	186.8	203.4	126.6	190.9	171.2	183.9
Av. ΣREE	37.84				112.42		78.45						174.23							
(La/Sm)cn	1.00	0.90	1.30	0.70	2.70	3.50	2.40	1.90	2.30	2.20	1.80	1.70	1.60	1.40	2.00	1.00	0.20	1.80	0.40	0.40
(Gd/Yb)cn	1.00	1.00	0.80	1.10	1.40	1.60	0.80	1.40	1.10	1.50	1.60	1.30	0.90	0.80	0.80	1.20	0.40	1.00	0.70	0.80
(La/Yb)cn	1.00	0.90	1.00	1.20	7.20	8.50	2.60	3.80	4.70	4.50	5.80	3.60	1.80	1.40	1.90	1.70	0.20	2.80	0.80	1.30
(Tb/Yb)cn	0.80	0.90	0.80	1.20	1.20	1.00	0.70	0.80	0.80	1.40	0.5	0.90	1.00	0.90	0.70	1.10	0.60	0.80	0.60	0.90
Eu/Eu*	0.60	0.60	0.50	0.60	0.80	0.90	0.30	0.60	0.60	0.50	0.70	0.40	0.10	0.10	0.10	0.1	1.90	0.20	1.50	1.20

Table 6: Fractionating modeling and mineral composition used in mass balance calculations (Wright and Doherty, 1970) for granodiorite and youngerer granite (monzogranite) of Gabal El-Gidami as one system.

Rock type	Major oxides	Observed daughter (S. No.7D	Observed Parent (S. No.10B)	Calculated Parent	Weighted residual	Fractionating phases (Deer *et al.*,(1966)					
						An37	Hb.	Bio.	Orth.	Qz.	Apt.
Monzogranite	SiO2	76.56	65.10	65.07	0.00	57.99	45.73	37.70	66.26	99.89	0.00
	TiO2	0.10	0.52	0.59	- 0.07	0.00	1.49	3.14	0.08	0.00	0.00
	Al2O3	12.33	16.57	16.56	0.00	26.39	11.39	14.60	20.39	0.03	0.00
	FeO*	1.14	5.52	5.51	0.01	0.19	16.44	30.22	0.16	0.09	0.22
	MnO	0.04	0.07	0.03	0.04	0.00	0.32	0.06	0.00	0.00	0.00
	MgO	0.13	1.10	1.10	0.00	0.03	10.58	4.23	0.10	0.00	0.53
	CaO	0.50	2.53	2.53	0.00	7.83	12.32	0.17	1.20	0.00	54.84
	Na2O	4.62	5.19	5.18	0.01	6.48	0.99	0.15	8.50	0.00	0.22
	K2O	4.60	3.45	3.45	0.00	1.10	0.78	8.25	3.32	0.00	0.00

Note that the analyses are recalculated to 100% and the total iron is given as FeO*. The composition of the fractionated phases (An37, Hb, Bio, Ortho., Qz. and Apt.) are from Deer *et al.,* (1966). Residual liquid (sample No. 7D)=12.04%, fractionating phases =87.96% (plagioclase 13.39%, hornblende 3.60%, biotite 15.23%, orthoclase 43.51%, quartz 11.80% and apatite 0.43%). The sum square of the residuals ($\sum R^2$) is 0.006.

Table 7: Fractionating modeling and mineral composition used in mass balance calculations (Wright and Doherty, 1970) for granodiorite and younger granite (syenogranite) of Gabal El-Gidami as one system.

Rock type	Major oxides	Observed daughter (S. No.16c)	Observed Parent (S. No.10B)	Calculated Parent	Weighted residual	Fractionating phases (Deer *et al.*,(1966)					
						An37	Hb.	Bio.	Orth.	Qz.	Apt.
Syenogranite	SiO2	77.21	65.10	65.07	0.00	57.99	45.73	37.70	66.26	99.89	0.00
	TiO2	0.06	0.52	0.58	- 0.06	0.00	1.49	3.14	0.08	0.00	0.00
	Al2O3	12.56	16.57	16.56	0.00	26.39	11.39	14.60	20.39	0.03	0.00
	FeO*	1.07	5.52	5.51	0.00	0.19	16.44	30.22	0.16	0.09	0.22
	MnO	0.01	0.07	0.02	0.05	0.00	0.32	0.06	0.00	0.00	0.00
	MgO	0.03	1.10	1.10	0.01	0.03	10.58	4.23	0.10	0.00	0.53
	CaO	0.48	2.53	2.53	0.00	7.83	12.32	0.17	1.20	0.00	54.84
	Na2O	4.06	5.19	5.18	0.01	6.48	0.99	0.15	8.50	0.00	0.22
	K2O	4.53	3.45	3.45	0.00	1.10	0.78	8.25	3.32	0.00	0.00

Note that the analyses are recalculated to 100% and the total iron is given as FeO*. The composition of the fractionated phases (An37, Hb., Bio., Ortho., Qz. and Apt.) are from Deer *et al.,*(1966). Residual liquid (sample No. 16C) = 10.72%, fractionating phases = 89.28% (plagioclase 11.94%, hornblende 3.69%, biotite 15.23%, orthoclase 46.01%, quartz 11.87% and apatite 0.52%). The sum square of the residuals ($\sum R^2$) is 0.007.

Conclusions

El-Gidami area lies in the Central Eastern Desert of Egypt, south Qena-Safaga road. Older granites (OG) and youngergranites are the main rock types in the study area. Chemical analyses of the whole-rock samples were carried out at ACME analytical Laboratories of Vandcouver, Canada. The OG is of tonalitic to granodioritic composition according to IUGS diagram with peraluminous nature and enriched in both Sr and Ba but depleted in Rb. The YGis monzogranite to syenogranite in composition with calcalkaline nature. Older granites and monzograniteare of I-type, whereas syenogranite is of A-type. REE diagrams showing positive Ce and negative Eu correlation, which may be due to the high value of Sr content; So the Eu is substituted by Sr cations (magmatic differentiation).

Fractional crystallization and mass balance modeling is used to calculate the amount of sum square of the residuals ($\sum R^2$). The calculation has been performed for granodiorite and monzogranite as one separate systemby fractional crystallization of plagioclase 13.39%, hornblende 3.60%, biotite 15.23%, orthoclase 43.51%, quartz 11.80% and apatite 0.43 %, then granodiorite and syenograniteas another separate system by fractional crystallization of plagioclase 11.94%, hornblende 3.69%, biotite 15.25%, orthoclase 46.01%, quartz 11.87% and apatite 0.52 % that gives a small value which indicate a good fit $\sum R^2$ (0.006). Also for granodiorite and syenogranite by fractional crystallization of plagioclase 11.94%, hornblende 3.69%, biotite 15.25%, orthoclase 46.01%, quartz 11.87% and apatite 0.52 % with 10.72% residual liquid sample (S.No. 16C). The relatively small value of $\sum R^2$ (0.007) indicates a good fit of the resulting model.

References

1. Abdel-Rahman, A. 1994. Nature of biotites from alkaline, calc-alkaline and peraluminous magmas. J. Petrol. 35 (2), 525-541.
2. Akaad, M.K., and Noweir, M.F., 1980. Geology and lithostratigraphy of the Arabian Desertorogenic belt of Egypt between latitudes 25˚ 30′ and 26˚ 30′ N, Jeddah, King Abdulaziz Unv, Inst. Apple. Geol. Bull. 3, 4, 127–135 p.
3. Barker, F., 1979. Trondhjemite: Definition, environment and hypotheses of origin. In: F. Barker (ed). Trondhjemite, Dacite and related rocks. Elservier, P.1-12. Barnes, H.L., ed., Geochemistry of hydrothermal ore deposits: New York, Holt, Rinehart, and Winston, Inc., p. 166–235.
4. Boynton, W.V., 1984. Geochemistry of rare earth elements: Meteorite studies. In: Henderson, P. (ed), Rare Earth Elements Geochemistry, Elsevier Pub. Co., Amsterdam, 63-114.
5. Condie, K.C. 1973. Archean Magmatism and Crustal Thickening. Geol.Soc. Amer. Bull., 84: 2981-2992.
6. Constantopoulos, J., 1988.Fluid inclusion and rare earth elements geochemistry of fluorite from South-Central Idaho. Economic Geology 83, 626-636.
7. Deer, W.A. Howie, R.A. and Zussman, J., 1966. An introduction to the rock forming minerals. London: Longman, 528p.
8. El-Gaby, S., 1975. Petrochemistry and geochemistry of some granites from Egypt. Neus Jb. Mineral, Abh. 124, 174-189 p.
9. El-Gaby, S., List. F. K., and Tehrany, R., 1988. Geology, evolution and metallogenesis ofthe Pan African belt of Egypt,In: El-Gaby and Greiling (eds), The Pan African Belt of Northeast African and Adjacent Areas; Tectonic Evolutionand Economic Aspects of Late Proterozoic Orogen, Friedr Vieweg and Sohn, Braunschweing / Wiesbaden, 17-67 p.
10. El- Ramly, M. F., 1972.A new geological map for the basement rocksin the Eastern and Southwestern Desert of Egypt, Scale 1: 100,000, Annals Geol. Surv. Egypt, 2, 1-18p.
11. El-Ramly, M. F., and Akaad, M. K., 1960. The basement complex in the Central Eastern Desert of Egypt, between lat. 24˚ 30′ and 25˚ 40′, Geo. Surv. Egypt, PaperNo. 8, 33p.
12. El Shatoury, H.M., Mustafa, M.E., Nasr, F.E., 1984. Granites and granitoid rocks in Egypt, a statistical approach of classification. Chem. Erde 43, 83-111.
13. El-Shazly, E. M., 1964. On the classification of the Precambrian and other rocks ofmagmatic affiliation in Egypt, U.A.R., Report presented insection 10, Int., Geol., Congr., India, 88–99 p.
14. Grommet L.P., and Silver L.T., 1983. Rare earth element distribution among minerals in a granodiorite and their petrogenic implications [J]. Geochemical Cosmochimica Acta.47, 925 - 939.
15. Gunther, J., Kleeman, M. and Twisted, D., 1989. The compositionally-zond sheet-like granite pluton of the Bushveld complex: Evidence bearing on the nature of A-Type magmatism. J. Petrol., 30: 1383-1414.
16. Henderson, P., 1996. Rare earth element, introduction and review. In: Rare earth element: Chemistry, origin and deposits. Edited by Jones, A.P.; Wall, F. and Williams, C.T., The Mineralogical Society Series, p.1-19.

17. Hermann A.G., 1970. Yttrium and lanthanides. In Handbook of Geochemistry (ed. Wedepohl), pp.39–57. Sprin. New York.
18. Irvine, T. N. and Baragar, W.R.A., 1971.A guide to the chemical classification of the common volcanic rocks. Can. Jour. Earth. Sc. 8,523-548p.
19. Kretz, R., 1983: Symbols of rock-forming minerals. American Mineralogist, 68, 277–279.
20. Middlemost, E.A.K., 1985. Magma and magmatic rocks. Longman group Ltd. London and New York, 75p.
21. Moghazi A. M, Mohamed F.H, Hassanen M.A. And Ali S., 2004. Late Neoproterozoic strongly peraluminous leucogranite, southeastern Desert, Egypt: petrogenesis and geodynamic significance [J]. Mineralogy and Petrology. 81, 19-41.
22. O' Connor, J.T., 1965. A classification of quartz-rich igneous based on feldspar ratio. U.S. Geol. Surv. Prof. Paper No. 528 B.P. 79-84.
23. Pearce, J.A. and Gale, G.H., 1984. Identification of ore deposition environment from trace element geochemistry of associated igneous host rocks. In: Volcanic process in ore gneiss. Inst. Min. and Metallurgy. Geol. Sec. London, Sepc. Publ. 7, 14-24.
24. Sabet, A.H., El Gaby. S., and Zalata, A. A., 1972. Geology of thebasement rockin the northern parts of El-Shayib and Safaga sheets, Eastern Desert,Egypt. Ann. Geol. Surv. Egypt, V.2, 111-128p.
25. Saleh G.M., Abd El Naby, H.H and Ibrahim, M.E., 2002. Granite magmatism in the Gabal Harhagit area, south Eastern Desert, Egypt: Characteristics and pathogenesis [J]. Egyptian J. of Geology. 46/1, 117 - 126.
26. Stern, R. J., and Hedge, C. D., 1985. Geochronologic and isotopic constraints on Late Precambrian crustal evolution in the Central Eastern Desert of Egypt. Am. J. sci. 285, 97-127p.
27. Streckeisen, A.L., 1976. Classification of the common igneous rocks by means of their chemical compositions. A provisional attempt. N. Jb. Min. Jour., 107,144-214.
28. Taylor, S. R. and Mclennan, S. M., 1985. The continental crust: its composition and evolution. Blackwell; p. 312.
29. Tuttle, O.F. and Bowen, N.L., 1958. Origin of granite in the light of experimental studies in the system $NaA1Si_3O_8$ - SiO_2 - H_2O. Geol. Soc. Amer. Mem., V. 74, P. 153.
30. Wright, T.L and Doherty, P.C., 1970. A linear programming and least squares computer method for solving petrologic mixing problems. Geol. Soc. Am. Bull., 81, 1995-2008.
31. El Mansi, M.M., 1993. Petrology, radioactivity and mineralizations of Abu Gerida El-Erediya area, Eastern Desert, Egypt. M.Sc., Fac. of Sci., Cairo Univ., p. 223.
32. Abu Dief, A., Ammar, S.E. Mohamed, N.A., 1997. Geological and geochemical studies of black silica at El-Missikat pluton, Central Eastern Desert, Egypt. Proc. Egypt. Acad. Sci. 47, 335-346.
33. Mousa, EMM. 2008. Post collisional A-type granites at missikate and Al Aradiya, Central Eastern Desert, Egypt, geochemical charachteristics and REE petrogenetic modeling 7th Inter Conf geochem. Alex. Univ., p.1-16.
34. Dardier, A.M., El-Galy, M.M., 2000. Contribution to the U-Th distribution in the older and younger granitoids along Qena-Safaga road, Central Eastern Desert, Egypt. Egypt. Jour. Geol. 44(1), 55-64.
35. Abd El Nabi, S.H., 2001. Evaluation of airborne gamma-ray spectrometric data for the Missikat uranium deposit, Eastern Desert, Egypt. Applied radiation and isotopes: including data, instrumentation and methods for use in agriculture, industry and medicine, 54, 497-507.
36. Abd El-Naby, H.H., 2007. Genesis of secondary uranium minerals associated with jasperoid veins, El Erediya area, Eastern Desert, Egypt. Mineral Deposite, 43, 933-944.
37. Dardier, A.M., 2004. Morphology, chemistry and U-contents of biotite flakes of the older granitoids and younger granites, Gabal El-Maghrabiya area, Eastern Desert, Egypt. Delta Jour. of Sci. 28, 1-18.
38. Hegazy, 2014. The application of Thermal Remote Sensing Imagery for studying uranium mineralization: A new exploratory approach for developing the radioactive potentiality at El-Missikat and El-Eridiya district, Central Eastern Desert, Egypt. P.53, 55-78.

6/28/2015